

# MEASURING MULTI-PHASE PARTICLE FLUX WITH A MULTI-FREQUENCY ACOUSTIC PROFILER

GW Wilson      Dalhousie University, Halifax, Nova Scotia, Canada  
AE Hay         Dalhousie University, Halifax, Nova Scotia, Canada

## 1 INTRODUCTION

Multi-frequency acoustic observations have been used in many laboratory and field studies to characterize the size and mass-concentration of oceanic sediments<sup>1-9</sup>, and to obtain simultaneous co-incident measurements of particle velocity<sup>10-12</sup>. The basis for this technique is inversion of a model for backscattered amplitude and phase; the most common model (the one used in all of the above studies) assumes particles within the measurement volume have narrow size- and velocity-distributions, an assumption which applies to a wide range of oceanic applications and hence has been very successful. This model does not apply to cases with bi-modal or multi-modal mixtures of particles types and/or sizes; such cases have not received as much attention in the oceanographic literature<sup>13</sup>, although there have been developments in other areas<sup>14</sup>.

This paper describes a laboratory experiment measuring the acoustic backscatter amplitude and phase from a bi-modal mixture of particles, using a multi-frequency pulse-to-pulse coherent Doppler sonar. An idealized case is considered: a mixture of strongly-scattering, slowly-moving polystyrene beads, and weakly-scattering, fast-moving glass beads, passively settling through water. It is hypothesized that independent information provided by different acoustic frequencies is sufficient to simultaneously infer the velocity and mass-concentration of each of the two particle classes. The use of nearly neutrally-buoyant polystyrene beads in this experiment is partly motivated by the idea that this technique could be used to measure the contrast between fluid and sediment velocities, which is relevant to theories for sediment mobilization and transport.

## 2 THEORY

### 2.1 Single-Mode Scattering

Consider a pulsed coherent sonar, which insonifies a small volume of randomly-distributed elastic scatterers at range  $r$  and at times  $t$  and  $t+\tau$ , and measures the amplitude  $V$  and relative phase shift  $\phi$  of the received (backscattered) pulses.

For suspended sediment transport, it is usually assumed that the scatterers are sediment particles, and that the relative spatial distribution of particles remains nearly constant within the interval  $\tau$ . In that case the measured phase shift,  $\phi$ , is proportional to the component of mean particle velocity parallel to the acoustic axis,  $U$ :

$$\phi = \frac{4f\tau}{c}U \quad (1)$$

where  $c$  is the speed of sound in water, and  $f$  is the acoustic frequency.

If it is further assumed that the particles are identical, their spatial distribution is random and uniform, and that multiple-scattering is negligible, the mean-square backscattered amplitude can be modeled as<sup>15-17</sup>

$$\langle V^2 \rangle = \frac{KB}{r^2} M e^{-4\alpha r}, \quad (2)$$

where  $K$  is a system sensitivity constant,  $M(r)$  is the mass-concentration of particles, and  $\alpha(f, r)$  represents the attenuation of sound due to water viscosity and scattering,

$$\alpha = \alpha_w(f) + \frac{A(f)}{r} \int_0^r M(r) dr. \quad (3)$$

The frequency- and grainsize-dependent coefficients  $B(f, a)$  and  $A(f, a)$  are related to the acoustic form factor and total scattering cross-section of the particles, as well as the particle diameter, and  $K(f)$  depends on properties of the transducer. These factors can be modeled under appropriate theoretical assumptions, but for brevity they are assumed to be known here.

## 2.2 Scattering from Distinct Particle Classes

The above model is now extended by relaxing the assumption that the particles are identical and moving with identical velocity. Instead, consider two classes of particle in suspension: each particle class  $i = 1, 2$  is assumed to be associated with a backscattering coefficient  $B_i$ , attenuation coefficient  $A_i$ , mass-concentration  $M_i$ , and velocity  $U_i$ , where the grainsize-dependence is now assumed implicit for each particle class.

With the same assumptions as above, equation (2) becomes

$$\langle V^2 \rangle = K \sum P_i^2 \quad (4)$$

where

$$P_i^2 = \frac{B_i M_i}{r^2} e^{-4\bar{\alpha} r}, \quad (5)$$

and

$$\bar{\alpha} = \alpha_w + \frac{\sum A_i}{r} \int_0^r M_i dr. \quad (6)$$

Assuming pulse-to-pulse coherent scattering for each particle class, the measured phase shift can be written using the identity for phasor angle addition,

$$\tan \varphi = \frac{\sum P_i \sin \varphi_i}{\sum P_i \cos \varphi_i}, \quad (7)$$

where

$$\varphi_i = \frac{4\pi \tau}{c} U_i. \quad (8)$$

Equations (4) and (7) comprise a model for the received backscatter and phase from a two-class particle suspension. Note, if  $B_i(f)$  and  $A_i(f)$  are known (e.g., based on calibration), then in principle an inverse problem can be posed to recover  $M_i$  and  $U_i$  from observations of backscatter amplitude and phase at two or more frequencies.

## 3 APPARATUS AND METHODS

An experiment was devised to collect acoustic measurements from a two-class particle mixture, using a settling column. The column, Figure 1, consists of a 1 m tall vertical section of 20 cm inside-diameter plastic (PVC) cylinder. Particles settle passively within the interior of the column, and are continuously recirculated (using a 12V bilge pump) from a collection cone in the bottom of the column. The particles re-enter the column via a diffuser near the top of the column. The entire apparatus is submerged in fresh water at 18.5° C. Water is allowed to freely flow through the top of the column, which is covered by a < 300 µm opening-diameter nytex mesh.

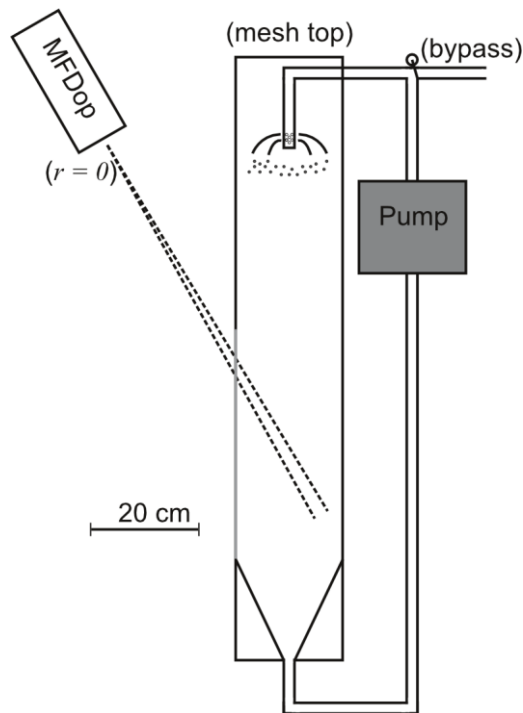


Figure 1: Diagram of settling column apparatus

In order to measure the total discharge through the column of each class of particle (denoted  $Q_i$ ), a bypass valve was installed in the recirculation circuit. This bypass was switched on at the end of each experimental run (i.e., after collecting acoustic data, see below), and triplicate samples of the pumped water-particle mixture were collected. The duration of each sample was determined by comparing the collected volume of water to a calibrated pump discharge rate. The total duration of sampling was chosen to be less than the time taken for a particle to settle through the column. The total discharge of each particle type was then determined by drying, separating and weighing the collected particles, and dividing by the sampling time.

Acoustic measurements were collected using a monostatic version of the MFDop<sup>18-19</sup>, a multi-frequency pulse-to-pulse coherent Doppler profiler. The MFDop transducer was mounted at an angle of 30 degrees relative to vertical, with the acoustic beam entering the column through a 43 cm tall by 5 cm wide window cut in the side of the column and covered with thin plastic. The range from the MFDop transducer face to the window was 49 cm.

In the present experiment, the MFDop was configured to transmit acoustic pulses of 5.25 µs duration at four acoustic frequencies in rapid succession, every 2 ms. Profiles of backscatter amplitude and pulse-to-pulse phase difference were collected as averages over 10 such pings, hence data were recorded at a rate of 50 Hz. Each experimental run consisted of four acoustic data collections of five minutes duration (14286 sets of 10-ping ensembles). Four unique acoustic frequencies were assigned to each collection, at 0.2 MHz spacing; in total, the measured frequencies ranged from 1.3 to 2.05 MHz, with a resolution of 0.05 MHz, which spans the nominal bandwidth of the transducer<sup>20</sup>.

The particles used in the experiments consisted of  $\sim 600 \mu\text{m}$  diameter polystyrene (Styropor) beads, and  $300\text{--}400 \mu\text{m}$  diameter soda-glass beads. The polystyrene beads were sieved to remove any beads of less than  $590 \mu\text{m}$  diameter, which resulted in a narrow size distribution; the glass beads were not sieved, and the stated diameter range is from the manufacturer (Ceroglass). A mixture of 5 g dry mass of polystyrene beads and 60 g dry mass of glass beads was used, which resulted in discharge rates in the settling column of  $Q_i = 0.046$  and  $2.6 \text{ g/s}$ , respectively. These bead types and mass ratios were chosen to obtain a large contrast in both acoustic scattering strength and settling velocity: the polystyrene beads are highly resonant at MHz frequencies<sup>21</sup>, and have nearly the same density as water ( $1055 \text{ kg/m}^3$ ).

## 4 RESULTS

Figure 2 shows backscatter amplitude and velocity from the MFDop measurements. Amplitude (measured in volts) was computed as the root-mean-square in range and time of the 10-ping-averaged data, multiplied by  $re^{2\alpha_w r}$  to correct for acoustic beam divergence and attenuation due to water. The time-averaged “velocity”  $w$  was computed as  $w = \bar{U} / \cos 30^\circ$ , where  $U$  is from equation (1), and  $30^\circ$  is the angle of the acoustic axis relative to vertical.

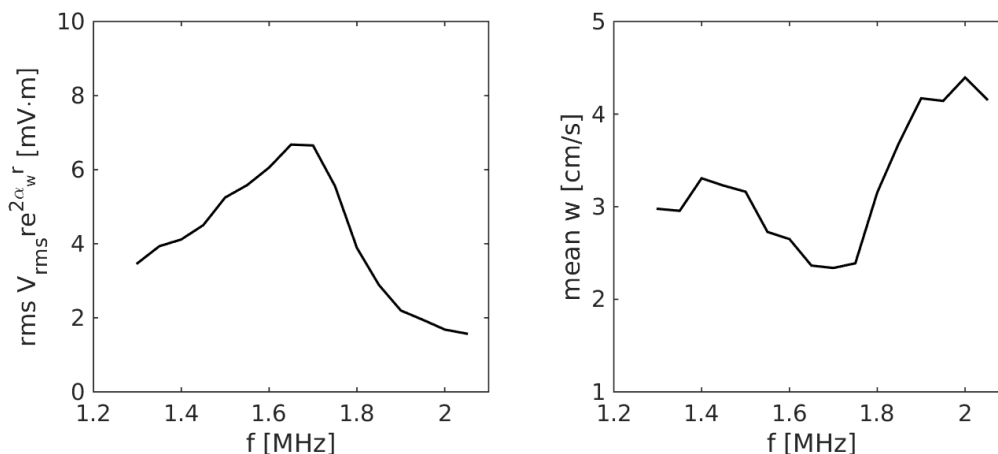


Figure 2: Observed root-mean-square (in range and time) backscatter amplitude (a) and mean vertical velocity (b) vs. frequency, for two-class particle settling experiment. Each class of particle is assumed to contribute to backscatter amplitude and phase (velocity) as in equations (4) and (7). The measured velocity  $w$  (b) is therefore frequency-dependent, unlike the case with a single particle class (equation (1)).

## 5 DISCUSSION

### 5.1 Backscatter Amplitude

The frequency-dependence of backscatter amplitude in Figure 2a is assumed to be mostly due to frequency-dependence in the coefficients  $B_i$  and  $A_i$  in equation (4). Note, system sensitivity  $K(f)$  also plays a role here, which is considered to be a secondary effect: the transducer is known to have maximum sensitivity at approximately 1.6 MHz, and the sensitivity is reduced by approximately 25% at  $\pm 0.4 \text{ MHz}$  around this center point.

Figure 3 shows a theoretical estimate of relative backscatter amplitude vs. frequency,

$$\frac{B_i}{K} = \frac{f_\infty^2}{\rho_s a} M, \quad (9)$$

where  $f_\infty$  is the backscatter form factor<sup>22</sup>,  $\rho_s$  is the particle density (2530 kg/m<sup>3</sup> for soda-glass, 1055 kg/m<sup>3</sup> for polystyrene), and  $a$  is the particle radius (estimated as 160 +/- 12.5 µm for glass beads, and 310 +/- 10 µm for polystyrene beads). The mass-concentration  $M$  was estimated using the measured discharge rates  $Q_i$ , divided by the Stokes settling velocity (8 cm/s for glass beads, 1 cm/s for polystyrene beads) times the cross-sectional area of the column. The resulting curves show the polystyrene beads are relatively stronger scatterers at  $f = 1.7$  MHz, whereas the two bead types have similar backscatter at frequencies greater than about 1.8 MHz. This qualitatively agrees with the shape of the measurements in Figure 2a.

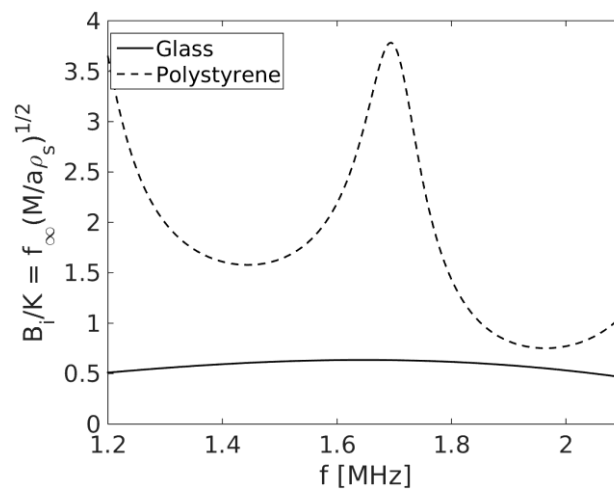


Figure 3: Theoretical estimate of relative backscatter amplitude for glass beads (solid line) and polystyrene beads (dashed line), using equation (9).

## 5.2 Velocity

For a single class of particles,  $w$  is expected to be independent of frequency, and equal to the settling velocity of the scattering particles. The measured  $w$  for this two-class particle suspension (Figure 2b) lies in-between the expected settling velocities for glass beads and polystyrene beads, as suggested by equation (7). A minimum in  $w$  was observed near  $f = 1.7$  MHz, consistent with the relatively larger backscatter amplitude of the slower-moving polystyrene beads at that frequency. Likewise, the measured  $w$  is largest near  $f = 2$  MHz, where scattering from the faster-moving glass beads is expected to be of the same order as from the polystyrene beads.

The clear frequency dependence of  $w$  (variations of more than 50%), combined with the frequency-dependence of backscatter amplitude, suggests information regarding the individual scattering phases might be extracted via equations (4) and (7). Future work will involve designing a calibration experiment for backscatter, and implementing an inversion scheme to test this hypothesis.

## 6 CONCLUSIONS

An experiment was conducted using a multi-frequency acoustic pulse-to-pulse coherent Doppler profiler to measure the backscattered amplitude and phase angle from a mixture of polystyrene beads and glass beads passively settling through water. The purpose of the experiment was to investigate the effect of the two particle classes on the multi-frequency measurements.

The results show that the presence of the slower-settling strongly-scattering polystyrene beads caused a reduction of measured phase, relative to that expected from the faster-settling weakly-scattering glass beads. This effect is measurably frequency-dependent, which suggests the possibility of model inversion to extract the velocity and mass-concentration of the separate particle classes. This suggestion is qualitatively supported by a model based on incoherent scattering theory.

## 7 REFERENCES

1. D. Hanes, C. Vincent, D. Huntley, T. Clarke, *Mar. Geol.* 81, 185–196 (1988).
2. C. E. Vincent, D. M. Hanes, A. J. Bowen, *Mar. Geol.* 96, 1–18 (1991).
3. A. E. Hay, J. Sheng, *J. Geo. Res.* 97, 15661–15677 (1992).
4. P. D. Osborne, C. E. Vincent, B. Greenwood, *Cont. Shelf Res.* 14, 159–174 (1994).
5. B. G. Ruessink et al., *J. Geo. Res.* 116 (2011).
6. R. B. O'Hara Murray, D. M. Hodgson, P. D. Thorne, *Cont. Shelf Res.* 46, 16–30 (2012).
7. T. Aagaard, *J. Geo. Res.* 119, 913–926 (2014).
8. P. D. Thorne, D. M. Hanes, *Cont. Shelf Res.* 22, 603–632 (2002).
9. P. D. Thorne, D. Hurther, *Cont. Shelf Res.* 73, 97–118 (2014).
10. L. Zedel, A. E. Hay, *JTECH* 16, 1102–1117 (1999).
11. D. Hurther, P. D. Thorne, M. Bricault, U. Lemmin, J.-M. Barnoud, *Coastal Eng.* 58, 594–605 (2011).
12. F. Pedocchi, M. H. Garcia, *Cont. Shelf Res.* 46, 87–95 (2012).
13. D. M. Hanes, *Cont. Shelf Res.* 46, 64–66 (2012).
14. X. Wu, G. L. Chahine, *J. Hyd., Ser. B* 22, 330–336 (2010).
15. A. E. Hay, *J. Geo. Res.* 88, 7525–7542 (1983).
16. A. E. Hay, *J. Acoustical Soc. Am.* 90, 2055–2074 (1991).
17. P. Thorne, C. Vincent, P. Hardcastle, S. Rehman, N. Pearson, *Mar. Geol.* 98, 7–16 (1991).
18. A. E. Hay, L. Zedel, R. Cheel, J. Dillon, *J. Geo. Res.* 117(C03005) (2012).
19. A. E. Hay, L. Zedel, R. Cheel, J. Dillon, *J. Geo. Res.* 117(C03006) (2012).
20. G. W. Wilson, A. E. Hay, *In Revision, Cont. Shelf Res.* (2015).